# The Effect of Microwave Irradiation on the Laser-generated Ag-$TiO_2$ Compound Nanoparticles

Abubaker H. Hamad†

Department of General Science, Faculty of Education, Soran University,
Kurdistan Region – F.R. Iraq

***Abstract*—The pulsed laser ablation technique in liquid solutions is a promising method for generating nanoscale materials due to its chemically clean and simple synthesis process. This study generates spherical Ag-$TiO_2$ compound nanoparticles (CNPs) through pulsed laser ablation, a picosecond (ps) laser, in deionized water. Then the spherical shapes of the CNPs are changed to rod-like shapes using microwave (MW) irradiation in an ordinary MW (continuous - CW) machine at 700 W for 3.5 min. The effect of MWs on the CNPs is investigated. Before and after MW-irradiation, the samples are characterised using ultraviolet-Vis Spectrometer, transmission electron microscope, and scanning electron microscope machines. The results show that the spherical shape of the nanoparticles was changed to rod-like shapes after MW irradiation. Their nominal dimensions range from 50–70 nm to 150–700 nm in width and length, respectively. Changing the morphology of the nanoparticles is important for various applications.**

***Index Terms*—Ag-$TiO_2$ compound nanoparticles, microwave irradiation, Nanoparticles, Nanorods, Picosecond laser, Rod-like shape.**

## I. Introduction

Microwave (MW) irradiation is not only used to synthesize nanoparticles but can also be used to manipulate the nanoparticles due to the high heating rates of MWs. Based on the literature review, MW irradiation has been used for the generation of ultrafine ZnO-NPs with controlled morphology (Hasanpoor, Aliofkhazraei and Delavari, 2015) and ultrafine silver nanoparticles (Ag NPs) (Saloga, Kästner and Thünemann, 2018), but not for manipulating nanomaterials. A MW was used to prepare rod-like shapes of AgNP@Ni-BTC nanocomposites (Amri et al., 2023). Different morphologies of Ag-NPs have been prepared through MW irradiation, such as sheets, wires, rods, and tubes (Kustov and Vikanova, 2023).

MW irradiation is used in nanotechnology. For example, ZnO-NPs are produced using a MW-assisted hydrothermal procedure. The nanoparticles have various sizes and shapes, such as flowers, needles, and spherical. It was concluded that by increasing the generation time from 10 to 15 min., needle-form nanoparticles at 50–150 nm were enhanced. On the other hand, flower-shaped nanoparticles were produced by increasing the power of the MW from 540 to 680 watts. In addition, ultrafine Ag-NPs (6 nm in size) were produced with MW irradiation assistance (Hasanpoor, Aliofkhazraei, and Delavari, 2015).

Not only does MW irradiation affect the nanoparticles' morphology, but post-irradiation by an unfocused laser beam irradiation significantly affects the manipulation of the nanostructure's morphology, size, and shape. Controlled MW irradiation has produced monodisperse aqueous emulsion droplets encapsulating spherical colloidal crystal particles. It was shown that the quality of packing of the colloidal crystal produced by this method can be used to show photonic energy band gap ($E_g$) characteristics (Kim et al., 2006). Laser and fluorescent (FL) irradiation were used for shape conversion of the Ag NPs, prepared by laser ablation in distilled water, from spherical to nanoprism, and nanorod crystal-shaped by NaCl (Tsuji et al., 2006). After that, (Al-Gaashani et al., 2011) showed the effects of the power of MWs on the morphology of the ZnO nanostructure. The spherical, needle-like, and leaf-like sheets were obtained at 450 W, 700 W, and 1,000 W MW powers. In addition, the average crystalline size of the ZnO nanostructures was changed from 32 nm to 17 nm when the power of the MW was reduced from 1,000 W to 150 W. In addition, Barreto, Morales, and Quintanilla (2013) have shown the effects of some experimental variables, including MW irradiation power, irradiation time, and temperature, on the morphology size and shape of ZnO-NPs produced through the MW-assisted approach. They concluded that these parameters significantly affect the morphology of the nanoparticles. MW-assisted was used to synthesize different kinds of metallic and metal oxide nanoparticles, including Ru-NPs (Gupta et al., 2013), CuO-NPs (Bekru et al., 2021), Ag-NPs (Quan et al., 2022), and compound nanoparticles (CNPs) like AgZnO-NPs (Porrawatkul et al., 2022).

This study generated the Ag-$TiO_2$ CNPs through a pulsed laser ablation technique in pure deionized water (DIW). A ps laser ablation was utilized to prepare the nanosize particles. Then, the as-synthesized nanoscale particles were irradiated through MWs in a MW oven. The shape of the nanoscale

ARO-The Scientific Journal of Koya University
Vol. XIII, No. 1 (2025), Article ID: ARO.11965. 6 pages
DOI: 10.14500/aro.11965
Received: 29 December 2024; Accepted: 28 March 2025
Regular research paper; Published: 06 April 2025
†Corresponding author's e-mail: abubaker.hamad@soran.edu.iq

 http://dx.doi.org/10.14500/aro.11965

particles changed from spherical to rod-like shapes with different dimensions. The novelty of this study is that for the 1st time, MW irradiation is used to manipulate the synthesized Ag-$TiO_2$ CNPs.

## II. Experimental Materials and Procedures

### A. Materials

To generate Ag-$TiO_2$ CNPs in DIW, a Ti: Ag bulk material was supplied by Cathay Advanced Materials Limited. The Ti: Ag ratio of the sample is 3:1 at%, and the purity of the elements of the alloy composite, Ti and Ag is 99.7%, and 99.95%, respectively. The dimensions of the compound material were (25 × 25 × 1) mm. The target material was cleaned about 3 times with DIW before starting and after finishing the ablation process. In addition, the target material was sonicated several times in an ultrasonic bath sonicator to remove any contamination on the target. An ordinary MW oven is used to post-irradiate the colloidal Ag-$TiO_2$ CNPs.

### B. Ag-$TiO_2$ CNPs Production Method

After washing the target material, it was put in a glass beaker (Pyrex) on a sample holder. The beaker was filled with DI water until the sample was completely immersed. It is worth mentioning that the DIW height was about 2 mm over the target material. The effect of water level on the laser power was taken into account.

To generate Ag-$TiO_2$ NPs, a 400-watt ps-laser (EdgeWave) was used. The bulk material was irradiated by the ps-laser for 10 min. with the following parameters (Table I).

### C. MW Irradiation of the as-synthesized Ag-$TiO_2$ NPS in a MW Machine

The synthesized Ag-$TiO_2$ CNPs (we named them As-synthesized Ag-$TiO_2$ nanoparticles - before MW irradiation) were irradiated by MWs in a MW machine at about 700 W for 3.5 min. The sample was placed at the center of the MW plate and rotated during irradiation. Due to vaporization, a reduction in the amount of as-synthesized Ag-$TiO_2$ nanoparticles was observed. The schematic diagram of the generation and MW irradiation of the nanoparticles by the laser ablation technique in DIW is depicted in the graphical abstract (Scheme 1).

### D. Sample Preparation for Nanoparticle Characterizations

Directly after the as-synthesized and post-irradiated samples were prepared, they were put in an ultraviolet (UV)-Vis spectrometer to measure their absorbance at different wavelengths. A standard Formvar/Carbon film supported copper microgrids size 200 mesh was utilized for transmission electron microscope (TEM) characterization. Some drops of the samples were carefully put onto a copper microgrid mesh and completely dried in the laboratory environment. For energy dispersive X-ray (EDX) analysis, several drops of the as-synthesized and MW-irradiated Ag-$TiO_2$ colloid were deposited above a normal glass substrate.

### E. Characterizations

The samples were characterized through different instruments. The absorption spectra of the samples (spherical, and rod-like shapes) in the form of colloidal nanoparticles were measured through a 250 dual-beam UV-Vis spectrometer (Analytic Jena). The size morphology was examined by a JEOL 2,000 TEM. The EDX machine, based on the X-ray technique, is used to identify all of the elemental compositions of the As-synthesized and MW-irradiated Ag-$TiO_2$ nanocomposites.

## III. Results and Discussion

### A. Generation of Ag-$TiO_2$ CNPs

Fig. 1 shows the TEM analysis of the as-synthesized Ag-$TiO_2$ CNPs. Based on our previous characterization; the smaller and larger nanoparticles are Ag-NPs and $TiO_2$-NPs, respectively. In addition, the darker areas of the nanoparticles are Ag-NPs, while the brighter nanoparticles are $TiO_2$-NPs (Hamad et al., 2015). The nanoparticles' shape is spherical. The smaller Ag NPs are attached to the larger titania nanoparticles. Ultrafine nanoparticles can be seen in the TEM images.

### B. MW Irradiation of the Ag-$TiO_2$ CNPs

Irradiation by MWs heats a target material throughout its entire volume instead of heating the whole surface area, and this property of MW irradiation makes the object heat faster and more efficiently than heating through conventional methods. In this work, after generating the nanoparticles by the ps-laser ablation technique, the nanoparticles were irradiated by MWs in an ordinary MW machine at about 700 W for 3.5 min.

Fig. 2a displays the UV-visible absorption spectra of the as-synthesized, and MW-irradiated Ag-$TiO_2$ samples. It can be seen that both absorption spectra have the same characteristics. A strong peak is observed from 210 nm to 260 nm of the wavelength, and an expanded peak is produced in the 400 nm to 500 nm wavelengths. Moreover, it can be noticed that the spectra of the MW-irradiated NPs are a little shifted to the longer wavelengths; this indicates that the larger Ag-$TiO_2$ particles are produced. It is worth mentioning that the TEM images confirm this result.

TABLE I
Parameters of the PS-Laser Utilized To Prepare Ag-$TiO_2$ CNPs in DIW

| Power (60%) (*W*) | Wavelength (λ) | Repetition rate (*f*) | Laser pulse duration (*τ*) | Beam spot size (D) | Beam scan speed (*v*) | Laser pulse energy (*E*) | Laser fluence ($F_L$) |
|---|---|---|---|---|---|---|---|
| 9.12 | 1064 nm | 200 kHz | 10 ps | 125 μm | 250 mm/s | 45.6 μJ | 0.37 J/cm$^2$ |

DIW: Deionized water

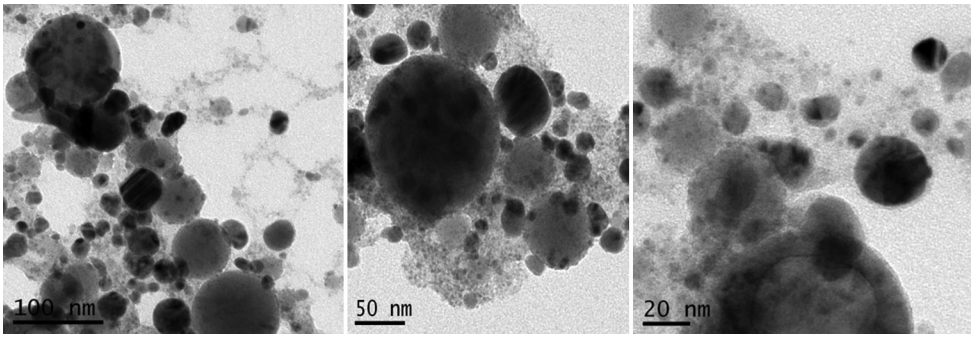


Fig. 1. Transmission electron microscope analysis of as-synthesized Ag-$TiO_2$ CNPs by ps-laser ablation technique through a picosecond laser in a liquid environment - DIW, (power, p = 9.12 Watts, repetition rate-frequency $f$ = 200 kHz, and beam scan speed $v$ = 250 mm/s).

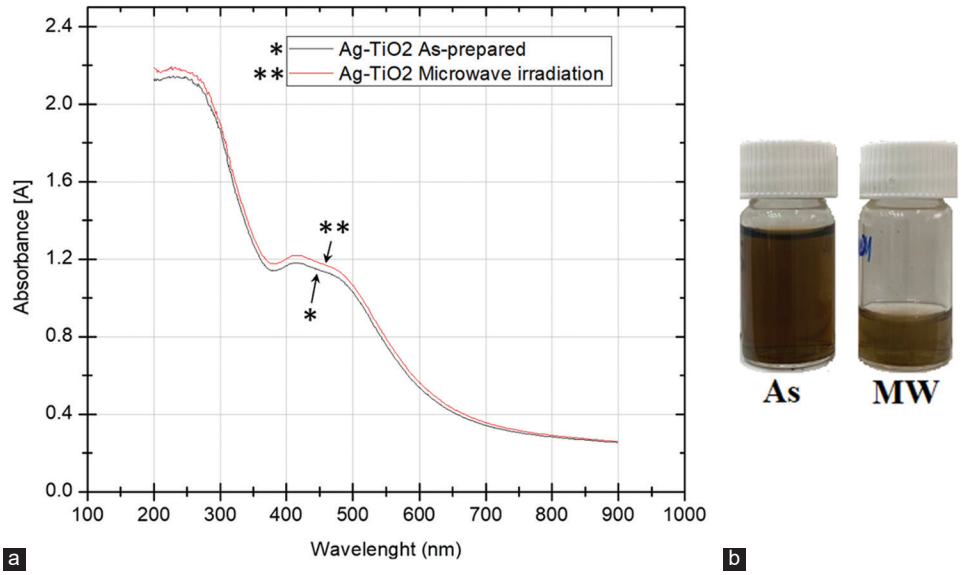


Fig. 2. (a) The ultraviolet-visible absorption spectra of as-synthesized or prepared (As) and microwave-irradiated (MW) Ag-$TiO_2$ samples. (b) The photographs show the real bottles of the as-synthesized (As) and microwave-irradiated (MW) colloidal Ag-$TiO_2$ samples.

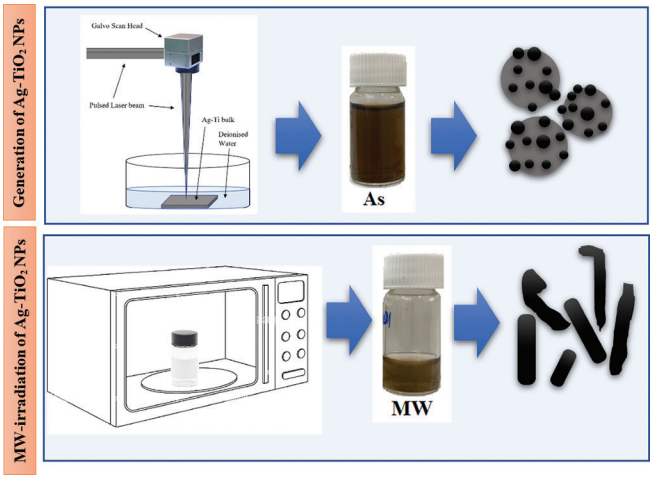


Scheme 1. Graphical abstract. An illustration of the generation and microwave irradiation of Ag-$TiO_2$ CNPs through ps laser in DIW.

The Ag-$TiO_2$ CNPs derived from the Ag: Ti bulk compound exhibit optical absorption spectra with a broad band ranging from 400 nm to 500 nm. The surface plasmon resonance of the Ag NPs in the compound is found within the 400 nm to 410 nm range; thus, any changes or shifts occurring in this peak do not appear.

Fig. 2b shows photographs of the bottles of the colloidal Ag-$TiO_2$ samples before and after MW irradiation. It can be noted that the amount of the colloidal nanoparticles after MW-irradiation (MW) is less than that of the as-synthesized (As) colloidal nanoparticles in the bottle due to the evaporation of the colloidal nanoparticles during MW irradiation in the MW oven.

Fig. 3 shows EDX analysis of the as-synthesized and MW-irradiated Ag-$TiO_2$ NPs. It can be noted that both spectra are approximately similar, except the peaks have different intensities due to the various amounts of nanoparticles on the glass substrate. As shown in Fig. 3, peaks associated with Ag, Ti, O, Na, Mg, Al, Si, and Ca are observed in the spectra. The Ti and O peaks confirm the existence of $TiO_2$-NPs, in addition, the Ti, O, and Ag peaks confirm the presence of Ag-$TiO_2$-NPs. The signals of Na, Mg, Al, Si, and Ca should be attributed to the building elements of the glass substrate. The spectra reveal that both samples have the same compositions; this is expected because the samples were not treated with any chemicals. Furthermore, compared with the

http://dx.doi.org/10.14500/aro.11965

As-synthesized spectrum, some small peaks of Ag and $TiO_2$ NPs do not appear in the MW-irradiated spectrum. This may be due to the crystallinity of Ag and $TiO_2$ NPs before and after the irradiation process, or it could be related to the low intensities of these peaks due to the small amount of nanoparticles in the prepared sample for characterization.

Fig. 4 displays TEM analysis of the MW-irradiated sample by MWs in an ordinary MW-oven at a power of about 700 Watts for 3.5 min. The figure shows that the morphology of the as-synthesized Ag-$TiO_2$ CNPs changed after MW irradiation from spherical shapes to almost rod-like shapes or belt-like shapes and some irregular shapes. It can be noted that rod-like shapes have dimensions of 50–70 nm and 150–700 nm in width and length, respectively. The first two rows of TEM images in Fig. 4 are almost rod shapes; however, the last two rows are almost random or uncontrolled rod-like shapes. The uncontrollable growth of the nanorods might be due to the interaction between the spherical nanoparticles and the MWs in the MW oven in all directions. In contrast, controllable or unidirectional growth of nanorods occurs in one direction. Although the radiation is uniform in the MW oven, the sample was rotated continuously during MW irradiation. It is worth mentioning that the quantitative analysis of the rod-like shapes was difficult due to the limited observation or scanning area on the TEM sample.

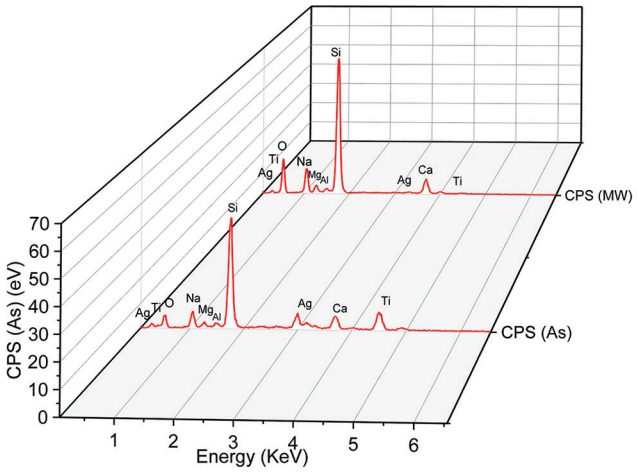


Fig. 3. Energy dispersive X-ray spectrum of the as-synthesized (As) and microwave irradiation (MW) Ag-$TiO_2$ samples.

The MW oven acts as a reactor, allowing it to turn or change the morphology of the nanoparticles through a reduction in reaction time (Saloga, Kästner and Thünemann, 2018). It is well-known that MWs can heat materials as a result of molecular vibration followed by a rise in temperature. The generated heat in the MW oven causes the temperature of the nanoparticles to rise below the melting point because the 700-watt power of the MW is approximately equivalent to 350°C. This degree of temperature is under the melting temperature of the Ag and $TiO_2$ nanoparticles, which are 961.8°C and 1843°C, respectively. The melting point of metals decreases when their size reduces (Feng et al., 2017).

Heat generation during MW irradiation is based on electromagnetic radiation through ionic conduction and dipolar rotation, which are directly related to reaction mixture composition. Thus, various chemical compounds have various MW absorbing properties, which allow the

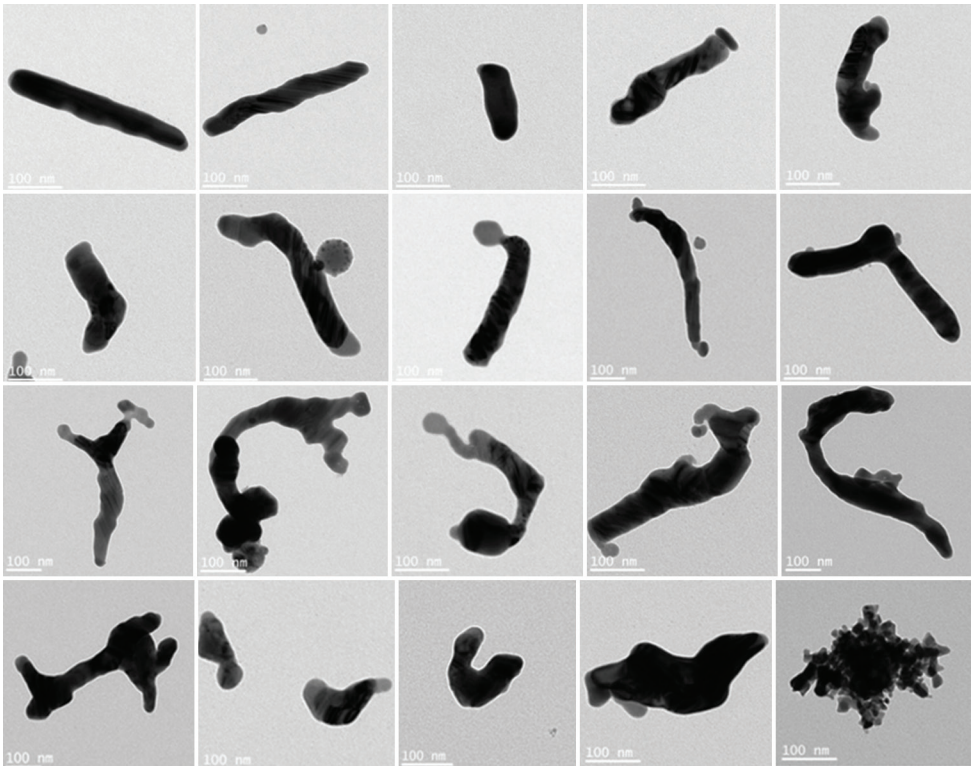


Fig. 4. Transmission electron microscope images of the Ag-$TiO_2$ rod-like shapes produced through microwave-irradiated Ag-$TiO_2$ CNPs by microwaves in an ordinary MW-oven at a power of about 700 Watts for 3.5 min.

heating of the chemical compositions in the reaction mixture (Barreto, Morales, and Quintanilla, 2013). The Ag and $TiO_2$-NPs have different abilities to absorb heat. As we know, the absorbed heat is related to the heat capacity of the materials; for example, the specific heat capacities of $TiO_2$-NPs and Ag-NPs are 686.2 J/kgK and 235 J/kgK, respectively (Tippa, Narahari, and Pendyala, 2016, Ahmed et al., 2018), thus, the higher specific heat capacity value means that it needs more energy to increase or decrease its temperature, while, a low value of the specific heat means that it does not need high energy to heat or cool down. As a result, the Ag-NPs absorb more heat than the $TiO_2$-NPs. This might cause Ag and $TiO_2$ NPs to change into nanorods in the solution. The shape transformation occurred with both Ag and $TiO_2$-NPs. As can be seen in Fig. 1, Ag and $TiO_2$-NPs have spherical shapes. The small-size Ag-NPs attached to the large-size $TiO_2$-NPs [12], while, Fig. 4, shows that both nanoparticles participated in the shape transformation because there are no spherical shapes just rod-like shapes of Ag-$TiO_2$ nanocomposites can be seen. In addition, the Ag-NPs and $TiO_2$-NPs became alloys in rod-like shapes.

Fig. 5 shows roughly measured lengths of the rod-like shape in a histogram. The major length of the rods is in the range of 300–400 nm, and the maximum length of the rod-like shapes is up to 700 nm. Based on the TEM analysis, the size of the Ag-$TiO_2$ CNPs ranged from a few nanometers to about 200 nm, and the average size was 31 nm.

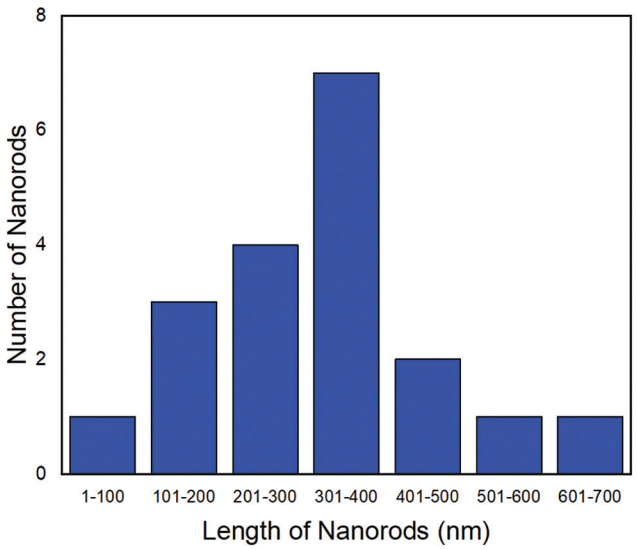


Fig. 5. Histogram of roughly measured the length of rod-like shapes.

## IV. Mechanism of Growth of Nanorod-Like Shapes

To elucidate the growing mechanism of nanorod-like shapes, it can be suggested that a bunch of spherical Ag-$TiO_2$ NPs in a specific area are combined, and then different shapes will be formed (Fig. 6). The rod-like shape formation from the nanoparticles is due to the direct effect of MWs on the spherical nanoparticles, which leads to the coalescence of some nanoparticles. First, the nanoparticles try to be close together due to the MW, which acts as a driving force at the beginning of irradiation. Then, the spherical nanoparticles can change into rod-like shapes through the coalescence process due to the continued irradiation. It can also be noted from the TEM images, that the growing process is random due to the MW irradiation process in different directions. It can be pointed out that the shapes of some nanoparticles remained unchanged after MW irradiation in the solution.

The TEM images of the nanocomposites shown in Fig. 7 support the above-mentioned mechanism of the formation and growth of rod-like shapes of the nanoparticles from spherical CNPs. These images were taken after post-irradiation of the CNPs in the MW oven. It can be noted in Fig. 7a and b that some nanoparticles are spherical, which means that they were not affected by MW irradiation. Some are changed to rod-like shapes, while some are in the coalescence process, which means between spherical and rod-like shape stages (Fig. 7c). Barreto, Morales, and Quintanilla (2013) concluded that an increase in MW power causes an increase in the temperature of the colloidal nanoparticles, which enhances the tendency of the nanoparticles to aggregate. Furthermore, the sample was rotated during the MW irradiation, some factors affect the shape conversion, such as the non-uniformly distributed temperature in the sample, or it may be due to the MW power induced to the center of the aggregated nanoparticles. As a result, less power reaches the nanoparticles located at the center of the aggregated nanoparticles. In this case, the MW power can disaggregate the aggregated nanoparticles but cannot change them to rod-like shapes. Wang, Liang and Geng (2009) have observed two different types of coalescence of the Au NPs, the first one is the “combination

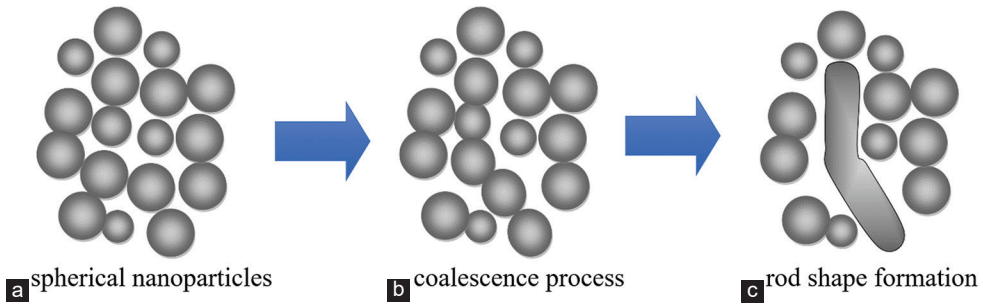


Fig. 6. (a-c) Possible mechanism of growth of the rod-like shape of the Ag-$TiO_2$ CNPs.

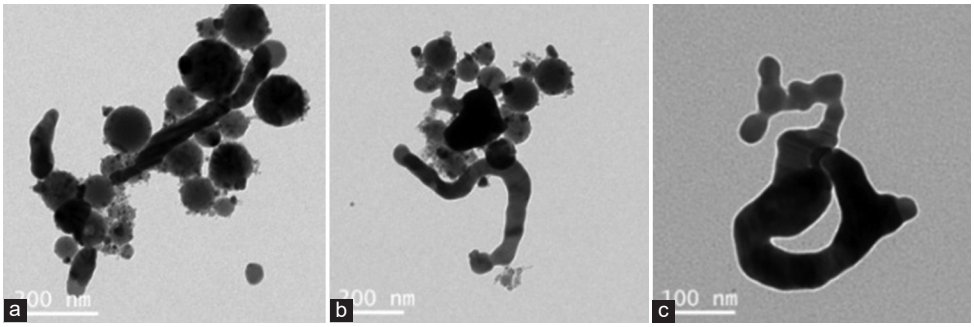


Fig. 7. Transmission electron microscope images of the growing steps of the Ag-$TiO_2$ nanocomposites: (a and b) spherical and rod-like shaped Ag-$TiO_2$ nanocomposites, (c) coalescence stage and rod-like shaped stage.

of two or more particles in appropriate orientations through twinning," and the second type is the "combination of two small particles with facets through a common lattice plane." (Wang, Liang and Geng, 2009). In addition, the molecular dynamic study showed that the coalescence process is affected by the size of the nanoparticles, the temperature of the nanoparticles, and the relative velocity of coalescence (Li, Hou and Wang, 2017).

## V. Conclusion

In the present study, MW-induced morphology change is investigated. A simple and effective MW irradiation technique has been utilized to change the morphology size of the as-synthetized Ag-$TiO_2$ CNPs from spherical to rod-like shapes. MW energy induces shape transformation in CNPs, leading to significant physical modifications. These findings in the shape modification of the Ag-$TiO_2$ CNPs can be applied to other types of compounds and non-CNPs.

## Acknowledgments

I would like to acknowledge and give my warmest thanks to Ms. Xiang Li Zhong at Manchester University who helped me with TEM characterization.

## References

Ahmed, S.E., Hussein, A.K., Mansour, M.A., Raizah, Z.A., and Zhang, X., 2018. MHD mixed convection in trapezoidal enclosures filled with micropolar nanofluids. *Nanoscience and Technology An International Journal*, 9, p.343.

Al-Gaashani, R., Radiman, S., Tabet, N., and Daud, A.R., 2011. Effect of microwave power on the morphology and optical property of zinc oxide nano-structures prepared via a microwave-assisted aqueous solution method. *Materials Chemistry and Physics*, 125, pp.846-852.

Amri, F., Kasim, W., Rochliadi, A., and Patah, A., 2023. Facile one-pot microwave-assisted synthesis of rod-like and hexagonal plate-like AgNP@ Ni-BTC composites for a potential salivary glucose sensor. *Sensors and Actuators Reports*, 5, p.100141.

Barreto, G.P., Morales, G., and Quintanilla, M.L.L., 2013. Microwave assisted synthesis of ZnO nanoparticles: Effect of precursor reagents, temperature, irradiation time, and additives on nano-ZnO morphology development. *Journal of Materials*, 2013, pp.1-11.

Bekru, A.G., Zelekew, O.A., Andoshe, D.M., Sabir, F.K., and Eswaramoorthy, R., 2021. Microwave-assisted synthesis of CuO nanoparticles using cordia africana Lam. Leaf extract for 4-nitrophenol reduction. *Journal of Nanotechnology*, 2021, pp.1-12.

Feng, D., Feng, Y., Yuan, S., Zhang, X., and Wang, G., 2017. Melting behavior of Ag nanoparticles and their clusters. *Applied Thermal Engineering*, 111, pp.1457-1463.

Gupta, S., Giordano, C., Gradzielski, M., and Mehta, S.K., 2013. Microwave-assisted synthesis of small Ru nanoparticles and their role in degradation of congo red. *Journal of Colloid and Interface Science*, 411, pp.173-181.

Hamad, A., Li, L., Liu, Z., Zhong, X.L., and Wang, T., 2015. Picosecond laser generation of Ag-$TiO_2$ nanoparticles with reduced energy gap by ablation in ice water and their antibacterial activities. *Applied Physics A*, 119, pp.1387-1396.

Hasanpoor, M., Aliofkhazraei, M., and Delavari, H., 2015. Microwave-assisted synthesis of zinc oxide nanoparticles. *Procedia Materials Science*, 11, pp.320-325.

Kim, S.H., Lee, S.Y., Yi, G.R., Pine, D.J., and Yang, S.M., 2006. Microwave-assisted self-organization of colloidal particles in confining aqueous droplets. *Journal of the American Chemical Society*, 128, pp.10897-10904.

Kustov, L., and Vikanova, K., 2023. Synthesis of metal nanoparticles under microwave irradiation: Get much with less energy. *Metals*, 13, p.1714.

Li, M., Hou, Q., and Wang, J., 2017. A molecular dynamics study of coalescence of tungsten nanoparticles. *Nuclear Instruments and Methods in Physics Research Section B: Beam Interactions with Materials and Atoms*, 410, pp.171-178.

Porrawatkul, P., Pimsen, R., Kuyyogsuy, A., Teppaya, N., Noypha, A., Chanthai, S., and Nuengmatcha, P., 2022. Microwave-assisted synthesis of Ag/ZnO nanoparticles using Averrhoa carambola fruit extract as the reducing agent and their application in cotton fabrics with antibacterial and UV-protection properties. *RSC Advances*, 12, pp.15008-15019.

Quan, M.X., Yao, Q.F., Liu, Q.Y., Bu, Z.Q., Ding, X.Z., Xia, L.Q., LU, J.Y., and Huang, W.T., 2022. Microwave-assisted synthesis of silver nanoparticles for multimode colorimetric sensing of multiplex metal ions and molecular informatization applications. *ACS Applied Materials Interfaces*, 14, pp.9480-9491.

Saloga, P.E., Kästner, C., and Thünemann, A.F., 2018. High-speed but not magic: Microwave-assisted synthesis of ultra-small silver nanoparticles. *Langmuir*, 34, pp.147-153.

Tippa, S., Narahari, M., and Pendyala, R., 2016. Unsteady Natural Convection Flow of Nanofluids Past a Semi-Infinite Isothermal Vertical Plate. In: *AIP Conference Proceedings*, AIP Publishing.

Tsuji, T., Okazaki, Y., Higuchi, T., and Tsuji, M., 2006. Laser-induced morphology changes of silver colloids prepared by laser ablation in water: Enhancement of anisotropic shape conversions by chloride ions. *Journal of Photochemistry and Photobiology A Chemistry*, 183, pp.297-303.

Wang, Y.Q., Liang, W.S., and Geng, C.Y., 2009. Coalescence behavior of gold nanoparticles. *Nanoscale Research Letters*, 4, pp.684-688.